

# Tranceive Phased Array with high Transmit Performance for Human Brain Application at 9.4 T

Nikolai I. Avdievich<sup>1</sup>, Andreas Pfrommer<sup>1</sup>, Jens Hoffmann<sup>1</sup>, Grzegorz L. Chadzynski<sup>1,2</sup>, Klaus Scheffler<sup>1</sup>, and Anke Henning<sup>1,3</sup>

<sup>1</sup>Max Planck Institute for Biological Cybernetics, Tübingen, Germany, <sup>2</sup>Department of Biomedical Magnetic Resonance, University Hospital Tübingen, Tübingen, Germany, <sup>3</sup>Institute for Biomedical Engineering, University and ETH Zurich, Zurich, Switzerland

**Introduction:** Despite the intrinsic advantages of ultra-high ( $\geq 7$  T) field (UHF) spectroscopic imaging (SI), increased SNR and spectral resolution, few studies have been reported to date. This limitation is largely due to  $B_1$  inhomogeneity and decrease in transmit (Tx) efficiency ( $B_1/\sqrt{kW}$ ) (1). Tx surface loop phased arrays combined with RF shimming have been shown to improve Tx performance and homogeneity for head imaging up to 9.4 T (2,3). However, often Tx-arrays are enlarged to fit SNR-optimized receive (Rx) arrays and, therefore, cannot satisfy requirements in high  $B_1$  and bandwidth for UHF SI. In this work we have developed a tight fit 400 MHz transceiver (Tx/Rx) head phased array to provide for efficient transmission.

**Methods:** The array consists of a single row with 8 (10 cm - length, 7.8cm - width) evenly spaced rectangular surface loops (Fig.1) and measures 20cm in width and 23 cm in height. It is shielded with a shield located 4 cm away. Experimental  $B_1$  maps were obtained using the AFI sequence (5) and a head/shoulder phantom (Fig.1) constructed to match tissue properties ( $\epsilon=58.6$ ,  $\sigma=0.64$  S/m) (3). Adjacent surface loops were decoupled using a resonance inductive decoupling (RID) method (4), which provided excellent decoupling ( $<-23$  dB between elements (Fig.2) and made it very suitable for pTx.  $Q_U/Q_L$  measured 4 to 6. All data were acquired on the Siemens Magnetom 9.4 T human imaging system. Simulations of SAR were performed using CST Studio Suite and the Virtual Family "Duke" model.

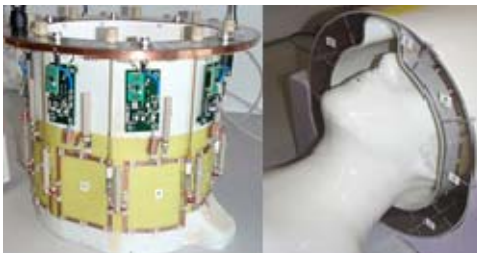


Figure 1: Layout of the 8-channel TX/RX coil.

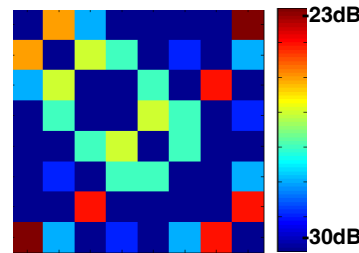


Figure 2: S12 matrix of the coil.

	$B_1^+$ Center	$\langle B_1 \rangle_{ax}^*$ Ax. Slice	Homog. STD, %	$\langle B_1 \rangle^*$ Head	SAR <sub>10g</sub> W/kg, max
Exp.	19.2	12.4	23	8.4	-
Sim.	20.3	13.9	18	9.6	4.33

\* $B_1$  values are presented in  $\mu T/\sqrt{kW}$ , SAR for  $P_{in}=8$  W measured at the coil.

Table 1: Experimental and Simulated Data

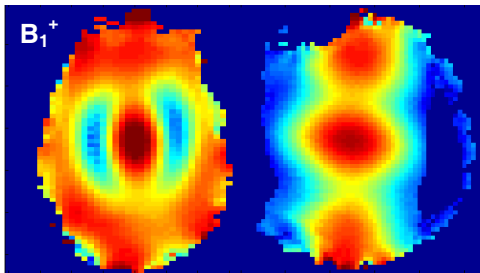


Figure 3: Experimental CP  $B_1^+$  maps (AFI) of a head-and-shoulder tissue dielectric phantom.

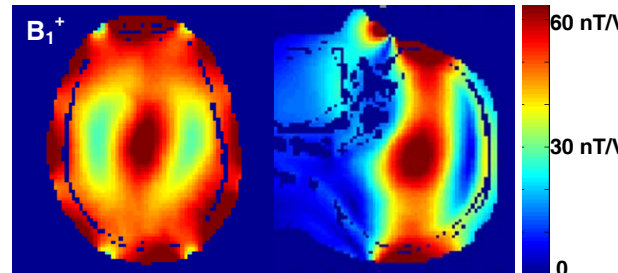


Figure 4: Simulated CP  $B_1^+$  maps of a human voxel model (CST). Figs. 3 & 4 are scaled identically.

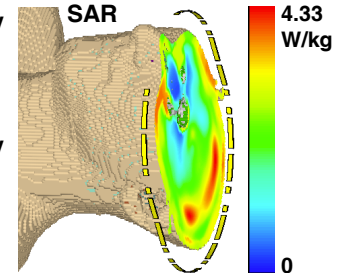


Figure 5: SAR simulation results for CP mode.

**Results:** The experimental  $B_1^+$  maps (Fig.3) measured with the array used in the CP mode are in accordance with the simulated CP  $B_1^+$  distribution (Fig.4). Figure 5 presents results of related SAR simulations. Table 1 summarizes all data. Tighter fit increases loading. Therefore, more energy is deposited into the sample and a high  $B_1^+$  efficiency is achieved. As seen from Figs. 3 and 4 the relative peripheral Tx efficiency in the axial slab through the phantom's center is also improved as compared with the common CP mode UHF  $B_1^+$  pattern produced by larger Tx coils (1-3), where peripheral  $B_1^+$  is substantially reduced compared to that in the center. As a result, the tight fit array improves the overall axial  $B_1^+$  distribution with elevated maximal and peripheral efficiency and improved homogeneity.  $B_1^+$  averaged over the central axial slice,  $\langle B_1 \rangle_{ax}$ , experimentally measured 55.6 nT/V as evaluated at the array input, which corresponds to 12.4  $\mu T$  per 1 kW of RF power delivered directly to the array. Homogeneity evaluated as a standard deviation over the central axial slice measured 23%. Simulations in the head model yielded similar results (Table 1). We also evaluated the local SAR distribution with maximal SAR<sub>10g</sub> measuring 4.33 W/kg when total 8 W delivered to the array input. Within the longitudinal coverage limited by the coil length the array also provided reasonably high SNR (Fig.3). However, the small number of array elements (8 elements) may limit the SNR and parallel Rx performance as compared with Rx-arrays with 30 and above elements (3). In the future we plan to develop a transceiver array with more channels for better SNR and coverage.

**Conclusions:** As a proof of concept we developed and constructed a tight fit 400 MHz 8-channel transceiver head phased array. The array provides high transmit efficiency and improved  $B_1^+$  distribution and homogeneity in the axial slab through the brain center. However, to further improve SNR and longitudinal coverage along the array axis, increasing the overall number of array elements is required.

**References:** 1) Vaughan JT et al, Magn. Reson. Med., 46:24-30, 2001. 2) Avdievich NI et al, Appl. Magn. Reson., 41(2):483-506, 2011. 3) Shajan G et al, Magn. Reson. Med., doi: 10.1002/mrm.24726. [Epub ahead of print]. 4) Avdievich NI et al, NMR in Biomed 2013, doi: 10.1002/nbm.2989. [Epub ahead of print]. 5) Yarnykh VL, Magn. Reson. Med., 57:192-200, 2007.